Split Frequencies in Planar Axisymmetric Gyroelectric Resonators

Sharif Iqbal Sheikh, Andrew A. P. Gibson, and Bernice M. Dillon

***Abstract*—Axisymmetric gyroelectric disk, ring, and composite resonator structures have been characterized for both InSb and GaAs semiconductors at 77 K. The calculations assume that these materials can be represented by the tensor permittivity derived from the Drude model of cyclotron motion in a plasma. Resonance and loss regions are identified and the sensitivity of normal mode splitting and onset frequencies to material and geometrical variables are graphed and tabulated. The information is presented in terms of signal frequency and the bias field to permit a direct comparison with results from ferrimagnetic structures. Semiconductor calculations show two extraordinary wave resonances and predict excellent symmetrical wide-band normal mode splitting. Field plots for the semiconductor disk and ring are included to explain coupled mode behavior between modes in different bias regions.**

***Index Terms*— Gyrotropism, resonators, semiconductor materials.**

I. Introduction

THE interaction of an alternating electric field with free carriers in a magnetically biased semiconductor produces gyroelectric cyclotron motion described by a tensor permittivity [1], [2]. This induces nonreciprocal propagation in magnetized structures and has potential applications in microwave and millimeter wave devices [3]. Many papers have appeared in the literature concerning the study of gyroelectric materials and propagation characteristics in semiconductor-filled rectangular [4], [5] and circular [6], [7] waveguides, multilayered [8], [9], and planar [10] structures. Currently, most interest is directed at integrating unidirectional lines and circulators in planar technology [11], [12]. This is particularly important above 40 GHz, where the gyromagnetic effect of ferrites becomes diminishingly small and losses in semiconductors are more acceptable. Before design techniques for ferrite circulators [13]–[15] can be extended to semiconductor materials, gyroelectric behavior of the modes in junction resonators have to be fully evaluated.

Axisymmetric geometries are the fundamental resonator shape employed in junction circulator design. Modal characteristics for both ferrite and semiconductor disks are calculated here using closed-form methods. Although the resonators exhibit duality in their classical tensor representation, once the material properties are introduced this duality is lost. Ferrites exhibit a single ferrimagnetic resonance whereas the Drude model of semiconductors predicts two extraordinary wave resonances. The most symmetrical wide-band split in ferrites occurs at frequencies below ferrimagnetic resonance, but in semiconductors excellent symmetrical splitting is predicted in the bias region that falls between the two extraordinary wave resonances.

Mode charts and selected field plots are also presented which describe how the normal modes split and tune with varying bias field in semiconductor ring and dielectric-semiconductor (DS) configurations. Differences in modal characteristics due to material properties are illustrated by comparing solutions for GaAs and InSb composite structures. The effect of geometrical and material variables on mode splitting and modal hierarchy is tabulated. The sensitivity to carrier concentration and effective mass indicates that accurate evaluation of material properties is essential to produce reliable mode charts for circulator design. Design techniques for practical semiconductor circulators have been previously published [12].

A. Solution of Axisymmetric Semiconductor Resonators

At microwave and millimetric frequencies a semiconductor immersed in a static magnetic-bias field exhibits a scalar permeability and a tensor permittivity $[\hat{\epsilon}_r]$ [1], [2]. When the bias field is in the axial $(\hat{z})$ direction this tensor has the form

$$[\hat{\epsilon}_r] = \begin{bmatrix} \epsilon & -j\eta & 0 \\ j\eta & \epsilon & 0 \\ 0 & 0 & \zeta \end{bmatrix}. \tag{1}$$

In planar structures only the $\mathrm{TE}_{\mathrm{nm}0}$ resonant frequencies are tuned and split by the gyroelectric properties described in (1). Closed-form methods [12]–[15] are widely used to study the $\mathrm{TE}_{\pm\mathrm{nm}0}$ modes which occur in configurations with magnetic top and bottom walls and electric sidewalls. The characteristic equation (CE) is obtained here by substituting the tensor permittivity into Maxwell's equations and imposing the required boundary conditions [16]. The CE for the $\mathrm{TE}_{\pm\mathrm{nm}0}$ modes associated with the two-region DS resonator, illustrated in Fig. 1, is given by (2), shown at the bottom of the next page, where the normalized wavenumbers are defined as $K_d = \omega\sqrt{\mu_o\epsilon_o\epsilon_d}$ and $K_o = \omega\sqrt{\mu_o\mu_r\epsilon_o}$. The relative permittivity of the nongyroelectric region is denoted by ϵ_d; $\epsilon_{\mathrm{eff}} = \frac{\epsilon^2-\eta^2}{\epsilon}$ and μ_r represent the effective permittivity and the relative permeability of the semiconductor, respectively. When $\epsilon_{\mathrm{eff}} < 0$, the nth-order Bessel functions J_n, Y_n and

Manuscript received December 5, 1996; revised October 9, 1997.

S. I. Sheikh is with the Islamic Institute of Technology, Gaziphur, Dakka, Bangladesh.

A. A. P. Gibson and B. M. Dillon are with the University of Manchester Institute of Science and Technology, Manchester M60 1QD, U.K.

Publisher Item Identifier S 0018-9480(98)00628-0.

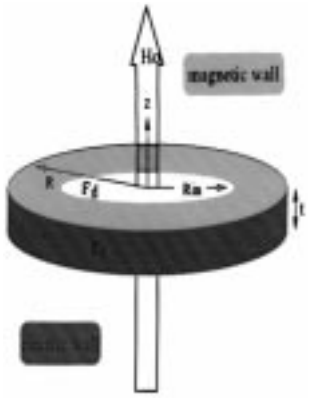

Fig. 1. Schematic diagram of planar axisymmetric dielectric semiconductor.

their derivatives in (2) are replaced by the appropriate modified Bessel functions and their derivatives.

For the homogeneous semiconductor disk with radius R, the above CE simplifies to one with two variables: the ratio of the tensor components (η/ϵ) and the normalized radial effective wavenumber $(K_{\text{eff}}R = K_o\sqrt{\epsilon_{\text{eff}}}R)$ [17]. The tensor entry solution of this fundamental axisymmetric geometry is depicted in Fig. 2. This graph is identical to the TM mode chart obtained for the dual ferrite disk geometry. It should be noted that the modal solutions are seemingly symmetrical about the demagnetized state $(\eta/\epsilon = 0)$ and the operating region is restricted to $|\eta/\epsilon| < 1$ with resonance regions occurring when $|\eta/\epsilon| > 1$.

B. Bias Field/Frequency Response

The practical design of semiconductor circulators requires a knowledge of mode splitting, resonance regions, and the onset frequencies of higher order modes in terms of the experimental variables of bias field and signal frequency. For homogeneous structures the tensor entry solution of Fig. 2 can be translated into the field/frequency domain. For inhomogeneous geometries the increased number of frequency-dependent parameters implies that the CE must be solved directly with bias field and frequency variables [18]. The next step, therefore, is to define the tensor constitutive components as a function of experimental and material properties.

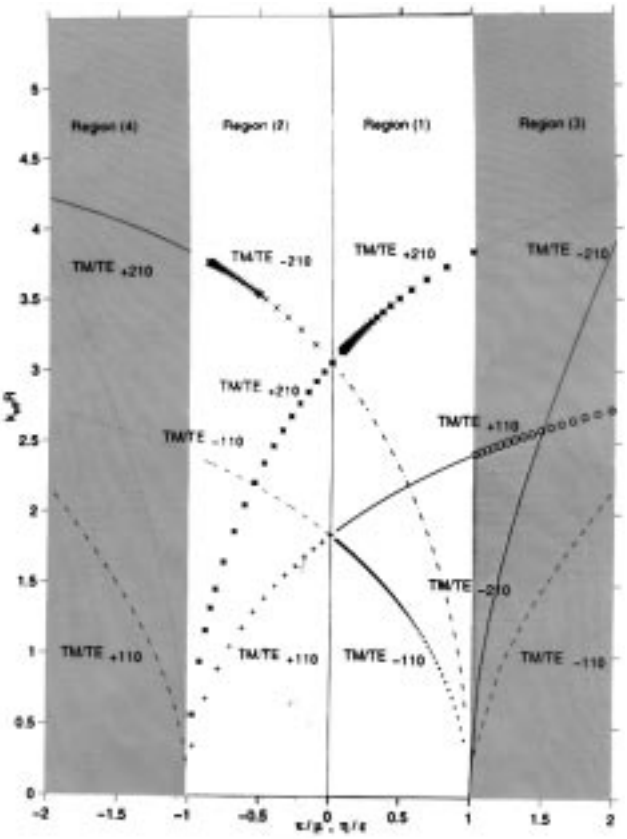

Fig. 2. Classical tensor entry solution of the cutoff planes of a planar resonator. Symbols used correspond to those of the modes in Figs. 4 and 5.

C. Material Properties

According to the Drude model [1] of magnetized semiconductors, the tensor entries are defined in terms of a dc permittivity (ϵ_r), the number of electrons per unit volume (N), collision frequency (ν_c), the charge of an electron (e) with effective mass m^*, signal frequency (f), and applied bias field (H_o). Thus $[\hat{\epsilon}_r]$ becomes (3), shown at the bottom of the page. Using (3), the effective permittivity (ϵ_{eff}) of a particular material can be calculated in terms of signal frequency and bias field [18]. Figs. 3(a) and (b) illustrates the real and lossy parts of ϵ_{eff} for a GaAs semiconductor

$$\left\{J_n'(K_oR\sqrt{\epsilon_{\text{eff}}}) + n\frac{\eta}{\epsilon}\frac{J_n(K_oR\sqrt{\epsilon_{\text{eff}}})}{K_oR\sqrt{\epsilon_{\text{eff}}}}\right\} - \left\{Y_n'(K_oR\sqrt{\epsilon_{\text{eff}}}) + n\frac{\eta}{\epsilon}\frac{Y_n(K_oR\sqrt{\epsilon_{\text{eff}}})}{K_oR\sqrt{\epsilon_{\text{eff}}}}\right\}$$
$$\cdot\left\{\frac{J_n'(K_dR_{\text{in}})J_n(K_oR_{\text{in}}\sqrt{\epsilon_{\text{eff}}}) - \sqrt{\frac{\mu_r}{\epsilon_d\epsilon_{\text{eff}}}}\left(J_n'(K_oR_{\text{in}}\sqrt{\epsilon_{\text{eff}}}) + n\frac{\eta}{\epsilon}\frac{J_n(K_oR_{\text{in}}\sqrt{\epsilon_{\text{eff}}})}{K_oR_{\text{in}}\sqrt{\epsilon_{\text{eff}}}}\right)J_n(K_dR_{\text{in}})}{J_n'(K_dR_{\text{in}})Y_n\left(K_oR_{\text{in}}\sqrt{\epsilon_{\text{eff}}}\right) - \sqrt{\frac{\mu_r}{\epsilon_d\epsilon_{\text{eff}}}}\left(Y_n'(K_oR_{\text{in}}\sqrt{\epsilon_{\text{eff}}}) + n\frac{\eta}{\epsilon}\frac{Y_n(K_oR_{\text{in}}\sqrt{\epsilon_{\text{eff}}})}{K_oR_{\text{in}}\sqrt{\epsilon_{\text{eff}}}}\right)J_n(K_dR_{\text{in}})}\right\} = 0 \quad (2)$$

$$[\hat{\epsilon}_r] = \begin{bmatrix} \left(\epsilon_r - \frac{Ne^2m^*(f-j\nu_c)}{f\epsilon_o[\{m^*(f-j\nu_c)\}^2-(e\mu_oH_o)^2]}\right) & -j\left(\frac{N|e^3|\mu_oH_o}{f\epsilon_o[\{m^*(f-j\nu_c)\}^2-(e\mu_oH_o)^2]}\right) & 0 \\ j\left(\frac{N|e^3|\mu_oH_o}{f\epsilon_o[\{m^*(f-j\nu_c)\}^2-(e\mu_oH_o)^2]}\right) & \left(\epsilon_r - \frac{Ne^2m^*(f-j\nu_c)}{f\epsilon_o[\{m^*(f-j\nu_c)\}^2-(e\mu_oH_o)^2]}\right) & 0 \\ 0 & 0 & \left(\epsilon_r - \frac{Ne^2}{f\epsilon_om^*(f-j\nu_c)}\right) \end{bmatrix} \quad (3)$$

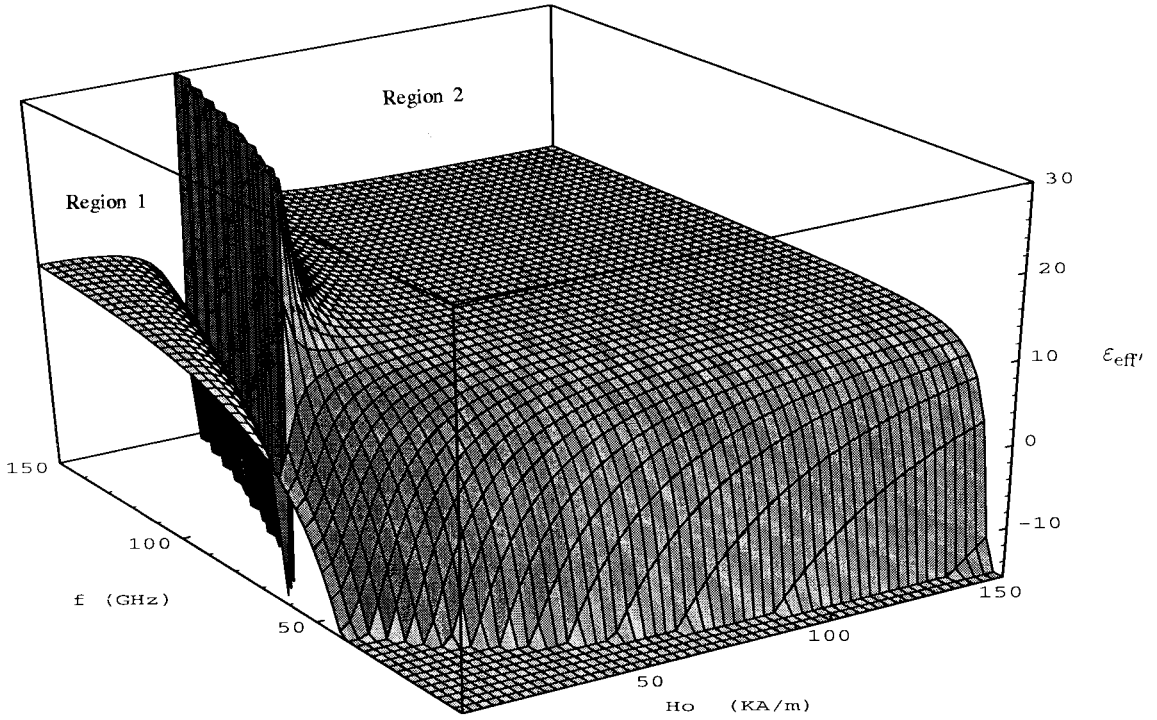

(a)

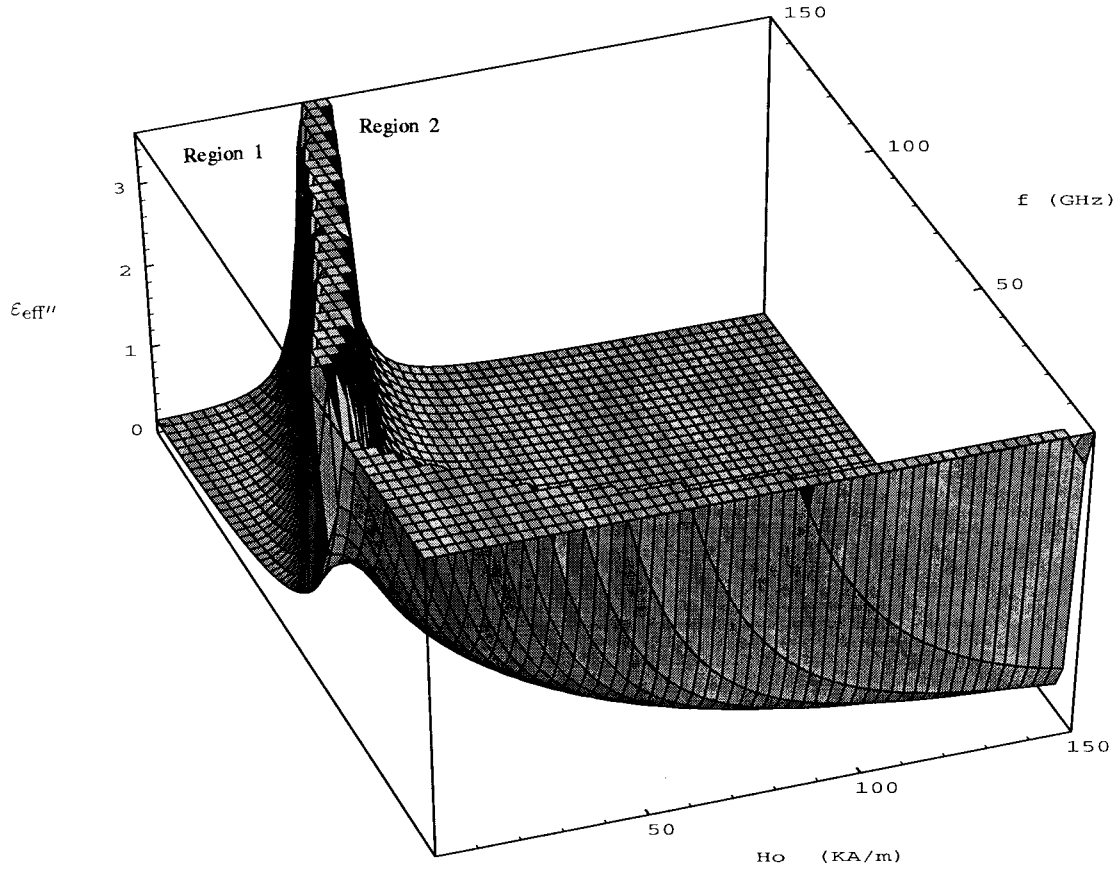

(b)

Fig. 3. Effective permittivity of a GaAs semiconductor. (a) $\varepsilon_{\mathrm{eff}'}$. (b) $\varepsilon_{\mathrm{eff}''}$.

TABLE I
ELECTRICAL PROPERTIES OF GaAs AND InSb AT 77 K

Material Properties	Gallium Arsenide ($GaAs$) at $77K$	Indium Antimonide ($InSb$) at $77K$
m^*	0.067	0.014
ϵ_r	12	16
N $(\frac{1}{m^3})$	10^{18}	10^{20}
ω_p $(\frac{rad}{sec})$	2.177×10^{11}	4.77×10^{12}

at 77 K and indicate the existence of two resonance regions associated with coupling to extraordinary waves. This is the gyroelectric equivalent of the ferrimagnetic resonance in ferrites. The resonance condition in semiconductors is associated with a singular value of effective permittivity ($\epsilon_{\text{eff}} \rightarrow \infty$). The losses in the resonance regions are proportional to the collision frequency. This ν_c term depends on the intrinsic carrier concentration, and so increasing temperature leads to increased losses, resulting in a broadening of the resonance regions. Table I summarizes the typical material properties used here for gyroelectric propagation in GaAs and InSb semiconductors.

The main operating region (Region 2) in Fig. 3(a) falls between the two extraordinary wave resonances and the subsidiary operating region (Region 1) occurs at frequencies above both these resonance regions. The gyroelectric effect of the material reduces when ϵ_{eff} approaches a constant value of (ϵ_r), with both increasing H_o in Region 2 and decreasing H_o in Region 1. In ferrites a similar analysis in terms of experimental parameters reveals only a single ferrimagnetic resonance [17]. This implies that the duality [16] between planar semiconductor and ferrite structures, described by normalized tensor entries, will not apply for solutions in terms of experimental and material parameters. Care, therefore, should be exercised in extending design procedures from ferrite to semiconductor devices.

D. GaAs Disk Resonator

A bias-field/frequency solution of a GaAs disk is obtained by substituting its material properties into (3) and then solving the characteristic equation (2) with the internal radius $R_{\text{in}} = 0$. The modal solutions illustrated in Fig. 4 predict excellent symmetrical splitting about the center frequency ($f = 26$ GHz for $\text{TE}_{\pm 110}$ mode) in Region 2, desirable in the design of planar-junction circulators. Useful split modes are also observed in the subsidiary operating region (Region 1) which occurs at lower bias fields. For comparison purposes, the mode chart for the classic nonreciprocal YIG–G113 disk [17] is reproduced in Fig. 5. In this gyromagnetic case, the modes below resonance (Region 2) exhibit more symmetrical wideband characteristics than those above resonance (Region 1). In semiconductors only, there exists an offset between the resonant frequencies associated with the limits of no bias

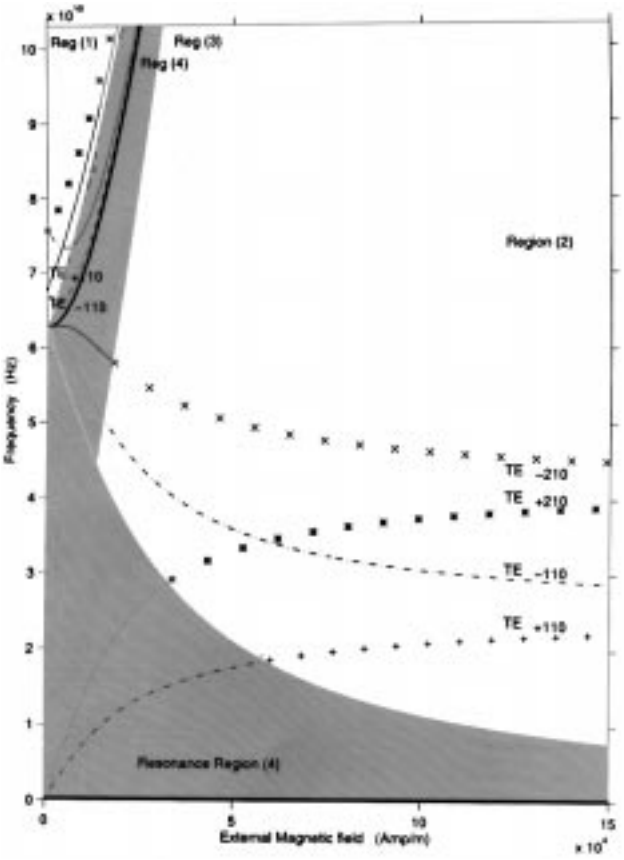

Fig. 4. Applied field/frequency solution of a homogeneous GaAs disk resonator for all the regions of magnetic bias. $N = 10^{18} 1/m^3$, $m^*/m_e = 0.067$, $\varepsilon_r = 12$, $v_c = 0$, $R = 1$ mm, $t = 0.1$ mm.

field and infinite bias field. This is due to the frequency dependence of ϵ_{eff} in the semiconductor, and the magnitude of this offset is material dependent. Table II summarizes the effect on frequency splitting and onset frequencies as the disk radius and semiconductor material constants are varied.

Each calculated point in Fig. 4 corresponds to a point in Fig. 2. The irregular spacing of the data is indicative of the nonlinear relationship between the tensor entry description and the applied field/frequency parameters. Although the solution in Fig. 2 is easier to calculate, the normalization parameters used distort the relationship between modes and regions. This normalization results in modal symmetry about the $\eta/\epsilon = 0$ axis of Fig. 2 which is not reflected in Fig. 4. Other examples of this distortion include $\text{TE}_{+\text{nm}0}$ modes which do not exist in Region 3 of Fig. 4, although this is predicted in Fig. 2; $\text{TE}_{-\text{nm}0}$ modes in Fig. 4 are calculated as a continuous function of H_o, whereas they cutoff at the resonance boundaries in Fig. 2. In view of these discrepancies due to the normalization, it is recommended that resonator characterization should be considered in terms of bias field and frequency.

E. GaAs Ring Resonator

Compared to disk structures, ring resonators provide additional geometric variables, flexibility, and opportunities for novel multiport components [19]. Fig. 6 depicts the mode chart for GaAs ring with metalized sidewalls and $R_{\text{in}}/R = 0.2$.

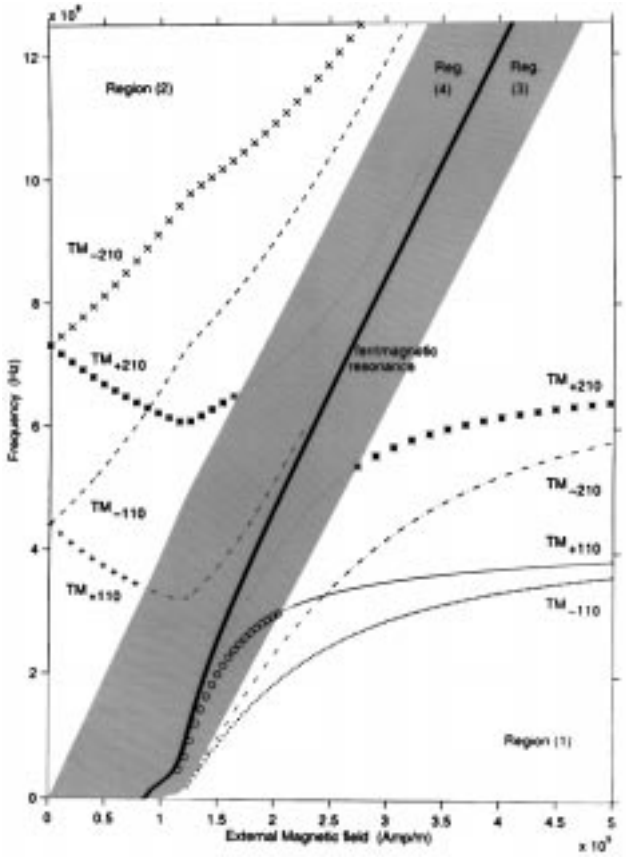

Fig. 5. Applied field/frequency modes of a homogeneous YIG–G113 disk resonator over the three regions of magnetization. $M_s = 140$ KA/m, $\varepsilon_r = 15.9$, $R = 5$ mm, $t = 0.1$ mm.

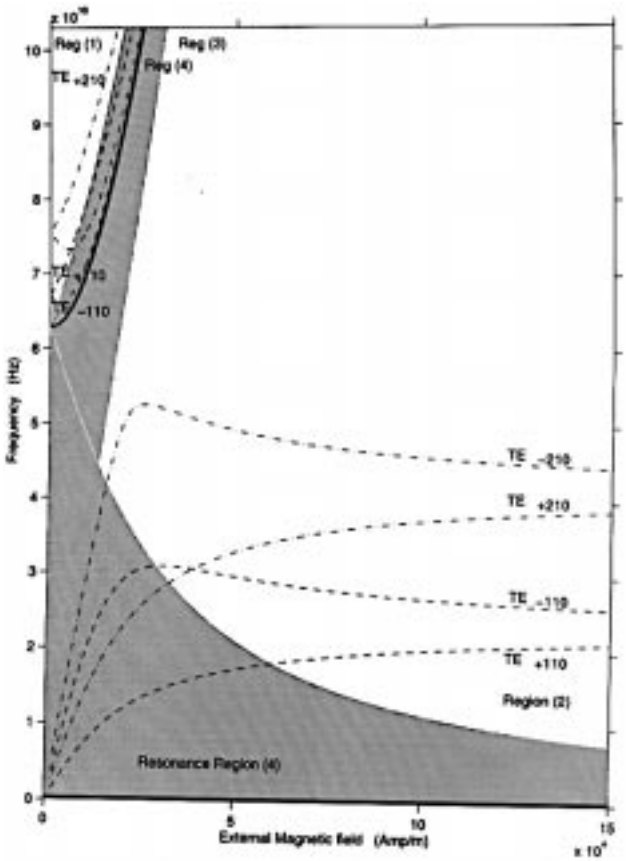

Fig. 6. Mode charts for homogeneous GaAs ring resonators with metalized sidewalls. $N = 10^{18}1/m^3$, $m^*/m_e = 0.067$, $\varepsilon_r = 12$, $v_c = 0$, $R = 1$ mm, $R_{\text{in}} = 0.2$ mm, $t = 0.1$ mm.

TABLE II
GEOMETRICAL AND MATERIAL EFFECTS ON THE MODAL BEHAVIOR OF MAGNETIZED SEMICONDUCTORS

GaAs non-reciprocal Disk Resonators				
Increasing value of :	Frequency Splitting		Onset Frequency	
	Region 1	*Region* 2	*Region*1	*Region*2
R_{out}	increases	reduces	reduces	
ϵ_r	reduces		reduces	
N	increases		reduces	increases
m^*	reduces		reduces	
GaAs non-reciprocal Ring and Composite Resonators				
R_{in}	reduces		reduces	
ϵ_d	increases		reduces	increases

Table II indicates that the onset frequency and the frequency splitting, i.e., difference frequency between the $\text{TE}_{+\text{nm}0}$ and $\text{TE}_{-\text{nm}0}$ modes, can be reduced by increasing the internal radius R_{in}. The behavior of the $\text{TE}_{\pm\text{nm}0}$ modes is similar to those of the disk, but a drawback of the ring is the reduction in the normal mode splitting (25% for the dominant mode at $H_o = 150$ KA/m). A contributory factor to this reduction is the convergence of the $\text{TE}_{-\text{nm}0}$ modes to zero cutoff in Region 4. This effect can be understood by comparing the field patterns of the disk and ring resonators. In Fig. 7(a) and (b), the transverse electric fields associated with the TE_{-110} modes in regions 1 and 2 occupies the inner and outer areas of the disk, respectively. In the ring geometry, the internal electric sidewall concentrates the electric field of the TE_{-110} mode in the same area of the semiconductor for both regions 1 and 2, as shown in Fig. 7(c) and (d). For this situation, coupled-mode theory [20] predicts greater coupling between the ring modes compared to those of the disk, thus, the TE_{-110} mode in Fig. 6 converges to zero cutoff. The same effect is also apparent for the TE_{-210} mode in Fig. 6.

F. GaAs and InSb Composite Resonators

Recent trends toward broad-banding and miniaturization of devices have led to interest in novel inhomogeneous junction resonators [21]. For inhomogeneous planar geometries, $\left(\frac{\eta}{\epsilon}, K_{\text{eff}}R\right)$ can no longer be used to characterize the modes because of the spatial variation in material properties. For axisymmetric composite DS resonators, (2) and (3) have four

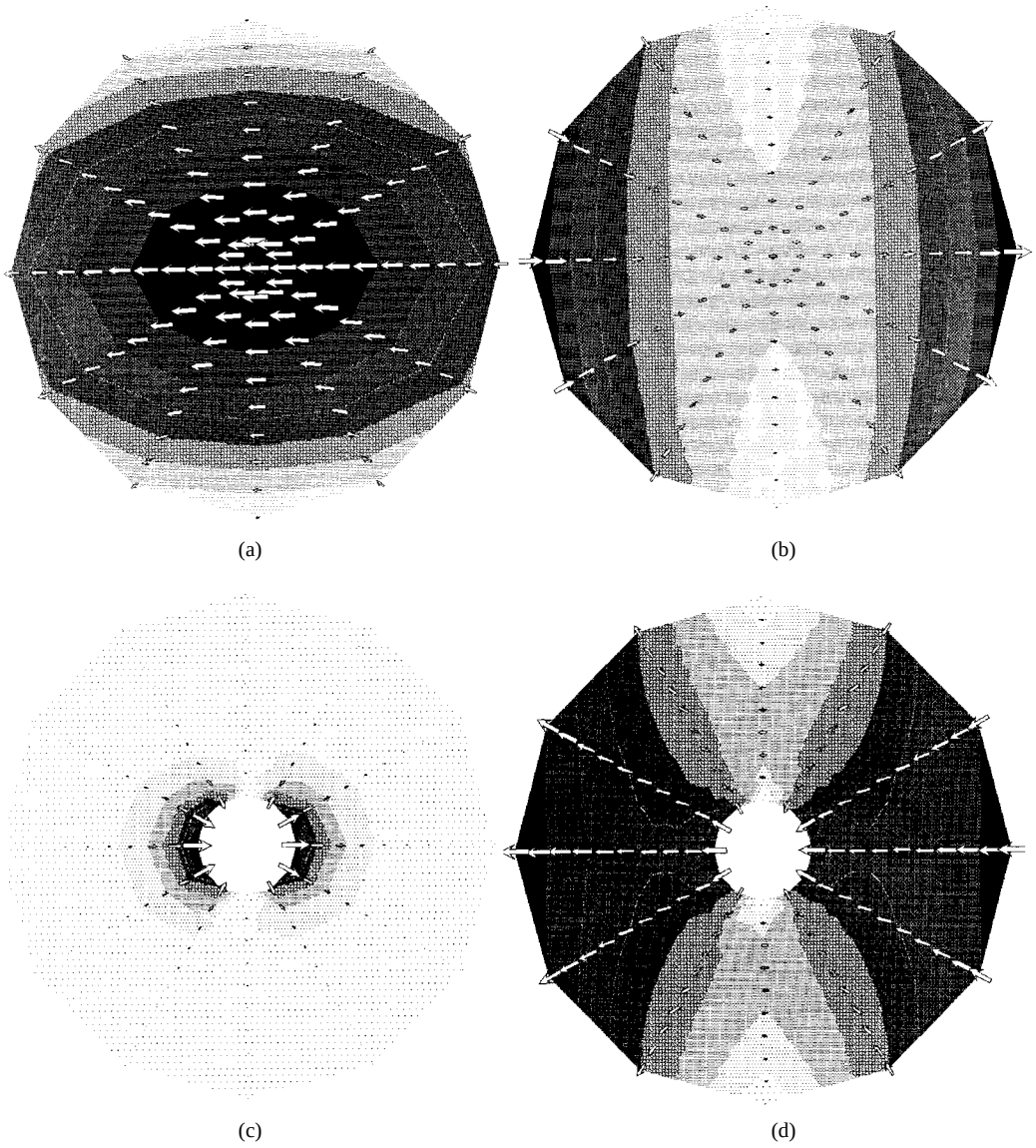

Fig. 7. TE field plots of axisymmetric nonreciprocal GaAs semiconductor resonators at (a) disk $H_o = 2$ kA/m, $f = 62.55$ GHz and (b) disk $H_o = 2$ kA/m, $f = 65.84$ GHz, (c) ring $H_o = 2$ kA/m, $f = 3.7$ GHz, and (d) ring $H_o = 2$ kA/m, $f = 65.89$ GHz.

frequency-dependent variables $(K_o, K_{\text{eff}}R, K_d, \eta/\epsilon)$ and a rigorous field/frequency solution becomes necessary. Fig. 8 illustrates the modal resonant frequencies of a magnetized GaAs–Air resonator at 77 K. This composite structure has similar characteristics to the disk with only a small reduction in the dominant $\text{TE}_{\pm 110}$ mode splitting, i.e., 6% at $H_o = 150$ KA/m. As shown in Table II, this reduction can be increased again by increasing ϵ_d.

The modal resonant frequencies of a magnetized InSb–Air resonator [18] at 77 K are shown in Fig. 9. In comparison with Fig. 8, the mode splitting and the modal hierarchy in Region 2 is largely unchanged. Compared to GaAs, InSb has an increased N and a reduced m^*. With reference to Table II, both these effects produce an increase in frequency splitting and override the reduction in frequency splitting due to the increased value of ϵ_r. These parameter changes also increase the plasma frequency $\left(\omega_p = \sqrt{\frac{Ne^2}{m^*\epsilon_o}}\right)$ in the InSb material, which results in an upward shift of the junction of the resonance region of 47%.

II. Conclusion

Major challenges in the practical implementation of semiconductor circulators include managing losses, validating the Drude model and implementing the electric sidewall boundary. A knowledge of the modal characteristics is also a prerequisite for determining the correct bias field and operating frequency. Magnetically tunable mode resonances in axially magnetized disk, ring, and composite resonators have been calculated. The tensor $\left(\frac{\eta}{\epsilon}, K_{\text{eff}}R\right)$ solution is obtained from the characteristic equation only, whereas the applied field/frequency solution requires the simultaneous solution of both the characteristic equation and the Drude model of material properties. The nonlinear relationship between these two formats has been examined—the bias field/frequency format is recommended to

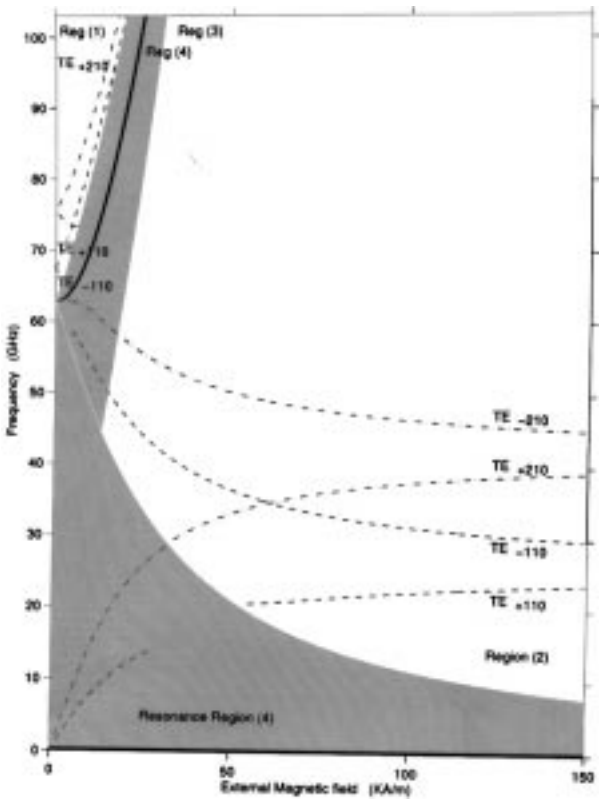

Fig. 8. Modal solutions of a GaAs–air composite planar resonator. $N = 10^{18}1/m^3$, $m^*/m_e = 0.067$, $\varepsilon_r = 12$, $\varepsilon_d = 1$, $v_c = 0$, $R = 1$ mm, $R_{\rm in} = 0.2$ mm, $t = 0.1$ mm.

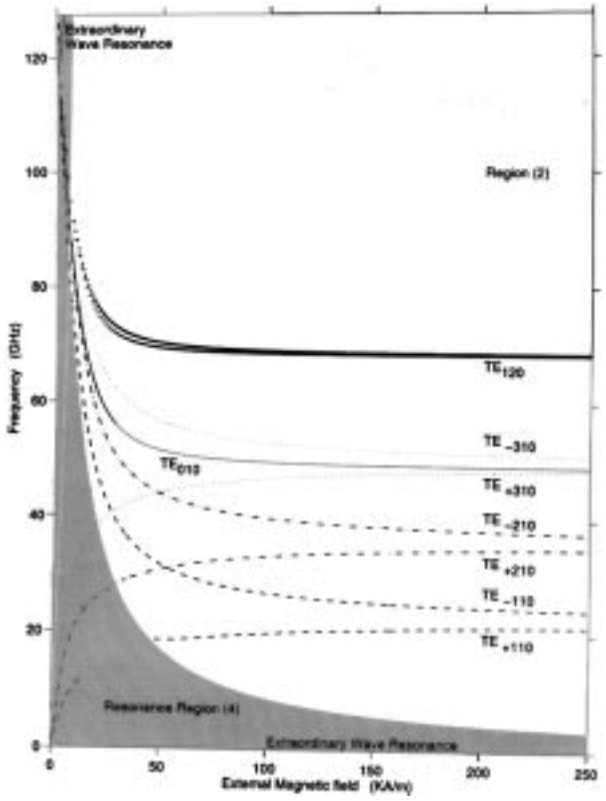

Fig. 9. Modal solutions of an InSb–air composite planar resonator. $N = 10^{20}1/m^3$, $m^*/m_e = 0.014$, $\varepsilon_r = 16$, $\varepsilon_d = 1$, $v_c = 0$, $R = 1$ mm, $R_{\rm in} = 0.2$ mm, $t = 0.11$ mm.

avoid the distortion introduced by the $\frac{\eta}{\epsilon}$ normalization. This distortion is compounded by the existence of two resonance regions in semiconductors compared to a single ferrimagnetic resonance. In ferrites, wide-band symmetrical splitting occurs below resonance, whereas in semiconductors excellent broadband splitting is predicted in the bias region that falls between the two extraordinary wave resonances. Thus, the characteristics of ferrite and semiconductors are significantly different in the field/frequency plane. The mode charts presented here provide guidance in the selection of bias field and operating frequency for planar, axisymmetric, and semiconductor junction resonators, and Tables I and II summarize their material and geometrical dependencies.

REFERENCES

[1] W. P. Allis, S. J. Buchsbaum, and A. Bers, *Waves in Anisotropic Plasmas.* Cambridge, MA: MIT Press, 1963.
[2] S. M. Sze, *Physics of Semiconductor Devices* (Interscience Series). New York: Wiley, 1969.
[3] "Special Issue on Gyroelectric Materials," *Proc. Inst. Elect. Eng.*, vol. 140, no. 3, pt. H, June 1993.
[4] N. H. Engineer, and B. R. Nag, "Propagation of electromagnetic waves in rectangular waveguides filled with a semiconductor in the presence of a transverse magnetic field," *IEEE Trans. Microwave Theory Tech.*, vol. MTT-13, pp. 641–646, May 1965.
[5] R. H. Sheikh and M. W. Gunn, "Wave propagation in a rectangular waveguide inhomogeneously filled with semiconductors," *IEEE Trans. Microwave Theory Tech.*, vol. MTT-16, pp. 117–121, Feb. 1968.
[6] V. I. Miteva and K. P. Ivanov, "Nonreciprocal effects in an azimuthally magnetized millimeter-wave solid-plasma circular guide," *Electron. Lett.*, vol. 23, no. 3, pp. 118–120, 1987.
[7] V. I. Miteva and K. P. Ivanov, "Some fundamental properties of azimuthally magnetized solid-plasma circuit guide," in *Proc. 19th European Microwave Conf.*, London, U.K., Aug. 1989, pp. 522–527.
[8] C. M. Krowne, "Electromagnetic theorems for complex anisotropic media," *IEEE Trans. Antennas Propagat.*, vol. AP-32, pp. 1224–1230, Nov. 1984.
[9] R. Pregla, "Method of lines for the analysis of multilayered gyrotropic waveguide structures," *Proc. Inst. Elect. Eng.*, vol. 140, no. 3, pt. H, pp. 211–218, June 1993.
[10] H. Baudrand, J. L. Amalric, E. L. Kanounl, and E. Badaouri, "Effect of surface admittance on non reciprocity in thick film InSb loaded slot line," in *Proc. 13th European Microwave Conf.*, Nurnberg, Germany, Sept. 1983, pp. 283–288.
[11] C. M. Krowne, A. A. Mostafa, and K. A. Zaki, "Slot and microstrip guiding structures using magnetoplasmons for nonreciprocal millimeter-wave propagation," *IEEE Trans. Microwave Theory Tech.*, vol. 36, pp. 1850–1859, Dec. 1988.
[12] L. E. Davis and R. Sloan, "Predicted performance of semiconductor circulator with losses," *IEEE Trans. Microwave Theory Tech.*, vol. 41, pp. 2243–2247, Dec. 1993.
[13] H. Bosma, "On stripline Y-circulation at UHF, *IEEE Trans. Microwave Theory Tech.*, vol. MTT-12, pp. 61–72, Jan. 1964.
[14] C. E. Fay and R. L. Comstock, "Operation of the ferrite junction circulator," *IEEE Trans. Microwave Theory Tech.*, vol. MTT-13, pp. 15–27, Jan. 1965.
[15] Y. S. Wu and F. J. Rosenbaum, "Wide-band operation of microstrip circulators," *IEEE Trans. Microwave Theory Tech.*, vol. MTT-22, pp. 849–856, Oct. 1974.
[16] A. A. P. Gibson, L. E. Davis, and S. I. Sheikh, "Dualities in circular gyrotropic disks and waveguides," *Electromagnetics*, vol. 15, no. 6, pp. 615–629, 1995.
[17] A. A. P. Gibson, B. M. Dillon, and S. I. Sheikh, "Applied field/frequency response of planar gyromagnetic disks," *Int. J. Electron.*, vol. 76, no. 6, pp. 1073–1081, 1994.
[18] S. I. Sheikh, A. A. P. Gibson, and B. M. Dillon, "Bias-field/frequency design charts for composite gyrotropic resonators," in *IEEE Symp. Microwave Theory Tech.*, San Francisco, CA, June, 1996, pp. 1663–1666.
[19] A. M. Borjak and L. E. Davis, "On planar Y-ring circulators," *IEEE Trans. Microwave Theory Tech.*, vol. 42, pp. 177–181, Feb. 1994.
[20] B. A. Auld, "Coupling of electromagnetic and magnetostatic modes in ferrite loaded cavity resonators," *J. Applied Phys.*, vol. 34, pp. 1629–1633, 1963.

[21] E. F. Schloemann, "Circulators for microwave and millimeter wave integrated circuits," *Proc. IEEE*, vol. 76, pp. 188–200, Feb. 1988.

Sharif Iqbal Sheikh was born on July 18, 1967, in Dhaka, Bangladesh. He received the higher secondary certificate (A level) degree from Notredame College, Dhaka, Bangladesh, in 1984, the B.Sc. degree in electrical engineering from Saint Carles University, Philippines, in 1990, and the M.Sc. and Ph.D degrees in electrical engineering from the University of Manchester Institute of Science and Technology (UMIST), Manchester, U.K., in 1992 and 1996, respectively.

He is currently working as an Assistant Professor in the Department of Electrical Engineering, Islamic Institute of Technology, Dhaka, Bangladesh.

Andrew A. P. Gibson was born in Dunfermline, Scotland, in 1962. He received the M.Eng. degree in electrical and electronic engineering and the Ph.D. degree from Heriot-Watt University, Edinburgh, Scotland, in 1985 and 1988, respectively.

He is currently a Senior Lecturer at the University of Manchester Institute of Science and Technology (UMIST), Manchester, U.K. His research has included finite-element analysis of gyromagnetic waveguides.

Dr. Gibson was the recipient of the 1985 Institution of Electrical Engineers (IEE, U.K.) Institute Prize.

Bernice M. Dillon received the B.A.I. degree in engineering from Trinity College Dublin, Dublin, Ireland, in 1984, and the Ph.D. degree from Cambridge University, Cambridge, U.K., in 1990.

From 1984 to 1986, she worked as a Design Engineer for Mentec Ltd., Dublin, Ireland. From 1991 to 1993, she was an SERC Post-Doctoral Fellow at the University of Manchester Institute of Science and Technology (UMIST), Manchester, U.K. Since 1993, she has been a Research Assistant at UMIST, working on various finite-element-based research projects.